Supporting Information For

Wood-based self-supporting Flexible Electrode Materials for Energy Storage Application

Linlin Liu[1]*, zhen ji[1], Shuyan Zhao[2], Qingyuan Niu[2], Songqi Hu[1]

1 Science and Technology on Combustion, Internal Flow and Thermo-Structure Laboratory, Northwestern Polytechnical University, Xi'an 710072, P. R. China

2 School of Material and Chemical Engineering, Zhengzhou University of Light Industry, Zhengzhou 450002, P. R. China

* Corresponding author.

E-mail: lll@nwpu.edu.cn

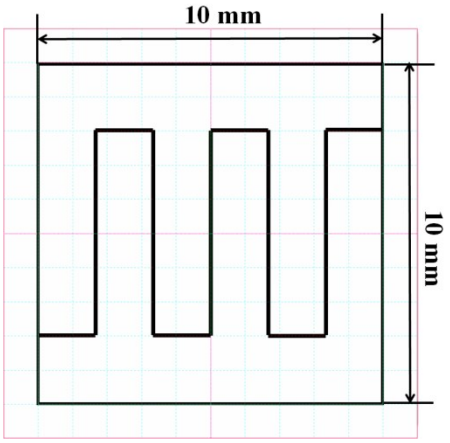

Fig. S1 The cutting path of CO_2 laser.

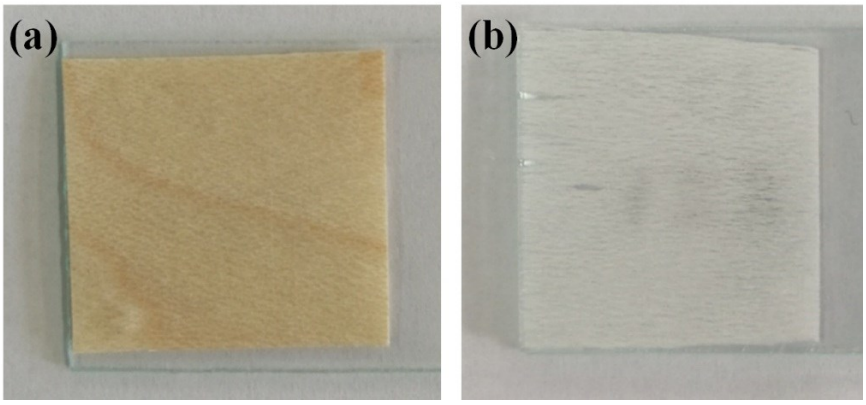

Fig. S2 Poplar wood slice (a) and the delignified poplar wood slice (b).

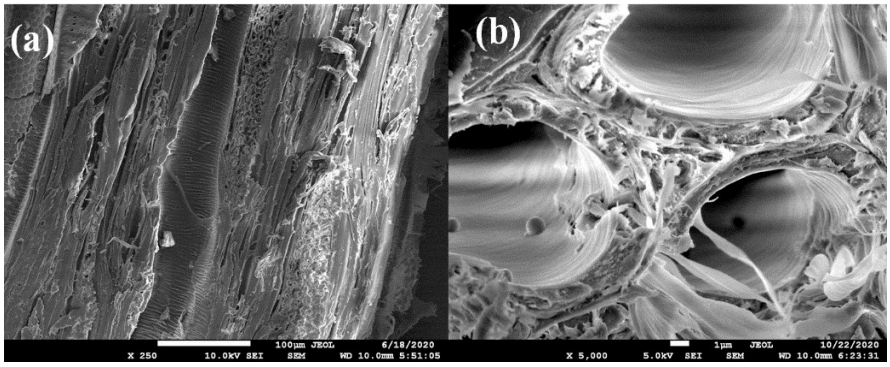

Fig. S3 SEM of the poplar wood slice: parallel to the growth direction (a) and perpendicular to the growth direction (b).

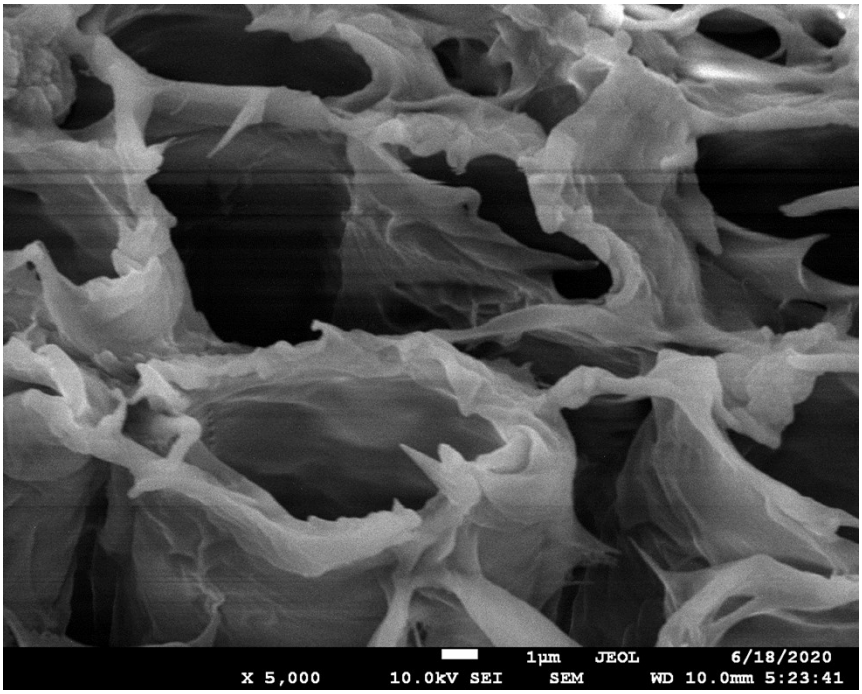

Fig. S4 SEM of the delignified poplar wood slice.

Table S1 Removal percentage of poplar wood.

	1 #	2#	3#	4#
poplar wood (g)	0.1752	0.1239	0.0985g	0.3976
Delignified poplar wood (g)	0.0798	0.0556	0.0371g	0.1725
Removal percentage of substances	54%	55%	62%	56%

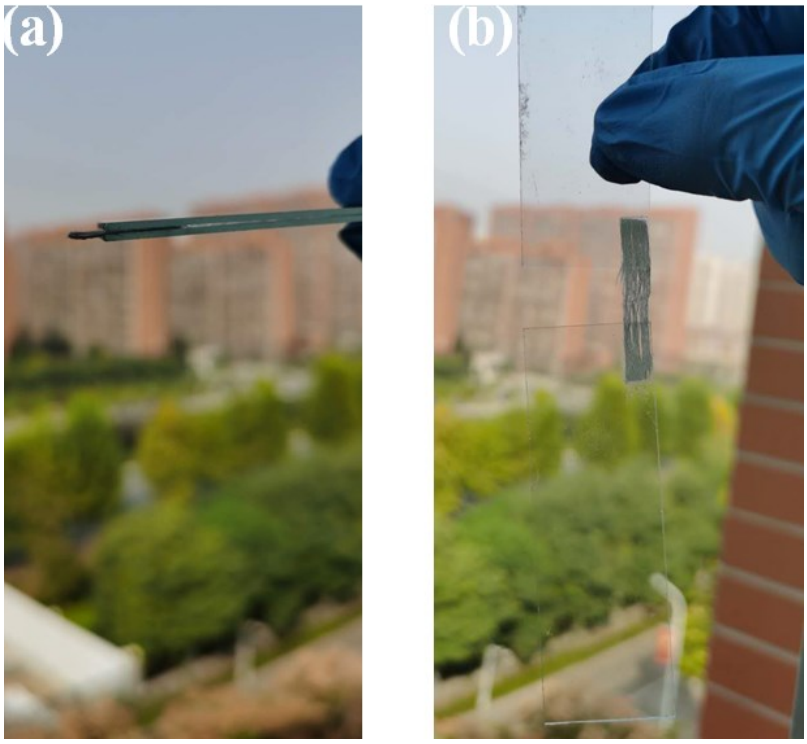

Fig. S5 Flexibility of the delignified poplar wood slice.

Table S2 Thickness of the delignified wood-based carbon material at different carbonization temperature.

Carbonization temperature (°C)	600	800	1000	1200
Thickness (μm)	41	40	51	53

Table S3 Carbon yield of the delignified wood-based carbon material at different carbonization temperature.

Carbonization temperature (°C)	600	800	1000	1200
Carbon yield (%)	23.18	22.12	19.73	18.62

Fig. S6 The DWFC-800 flexible electrode material.

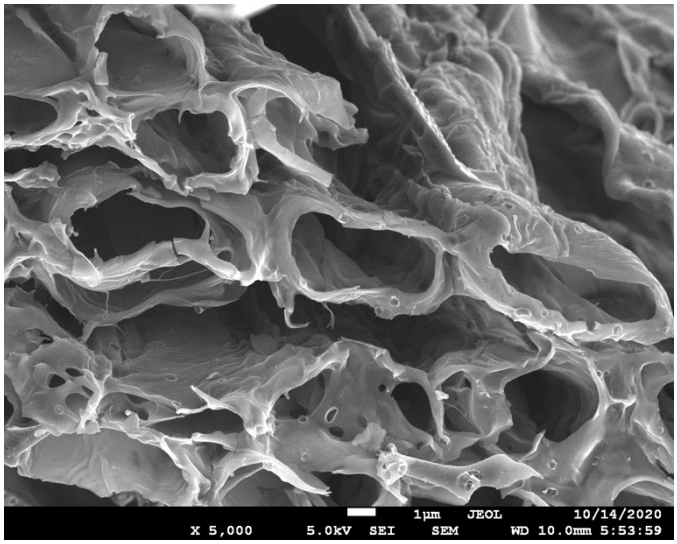

Fig. S7 SEM of the DWFC-800 flexible electrode material.

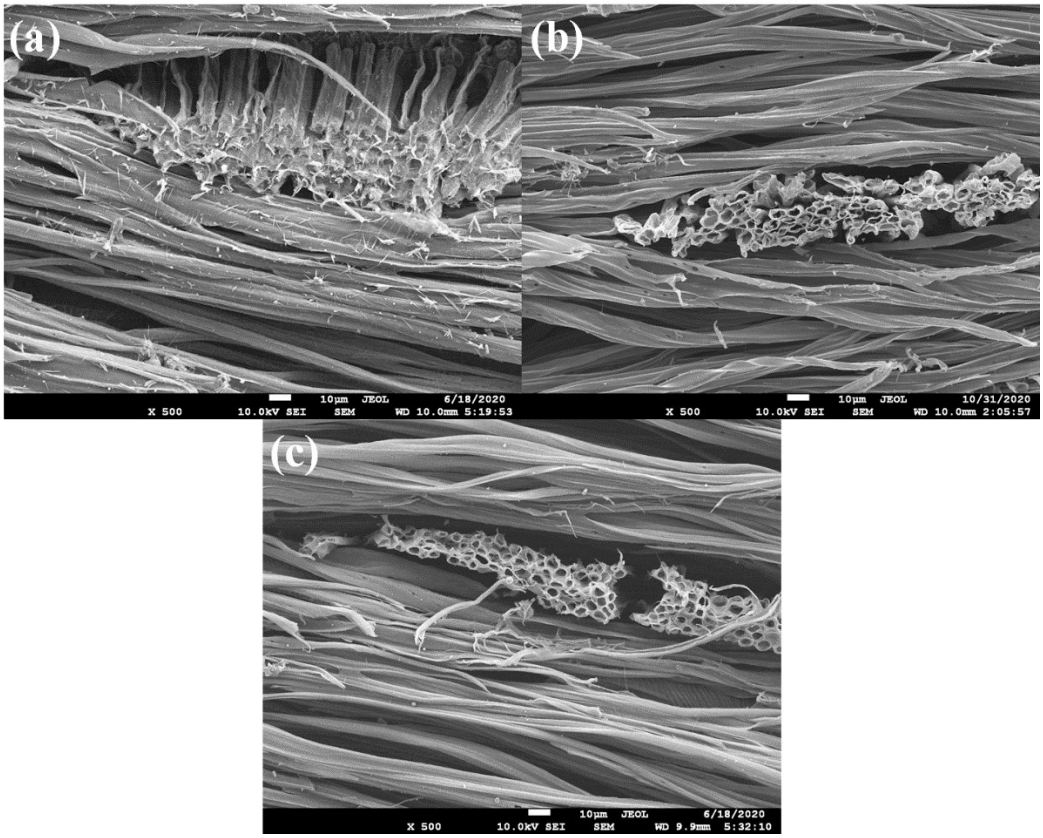

Fig. S8 SEM of the DWFC-600 (a), DWFC-1000 (b) and DWFC-1200 (c) flexible electrode material.

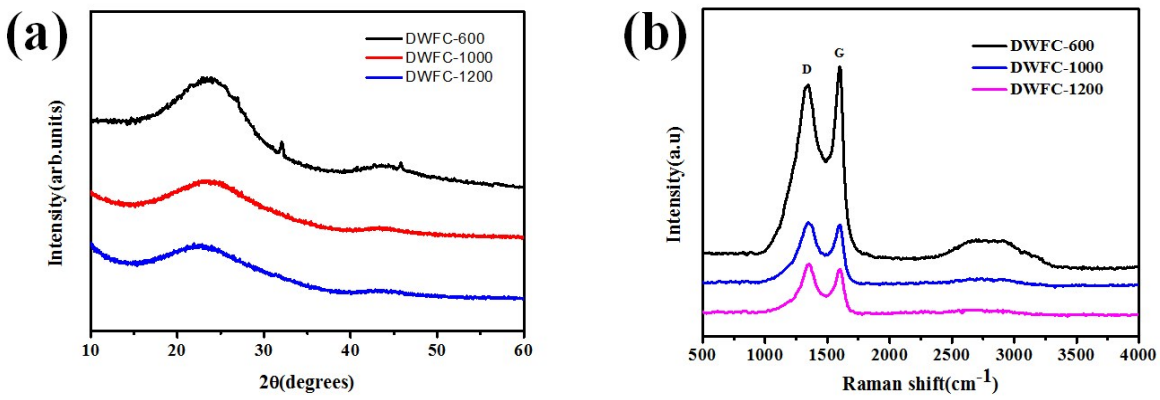

Fig. S9 The XRD pattern (a) and Raman spectrum (b) of the DWFC-600, DWFC-1000 and DWFC-1200 flexible electrode material.

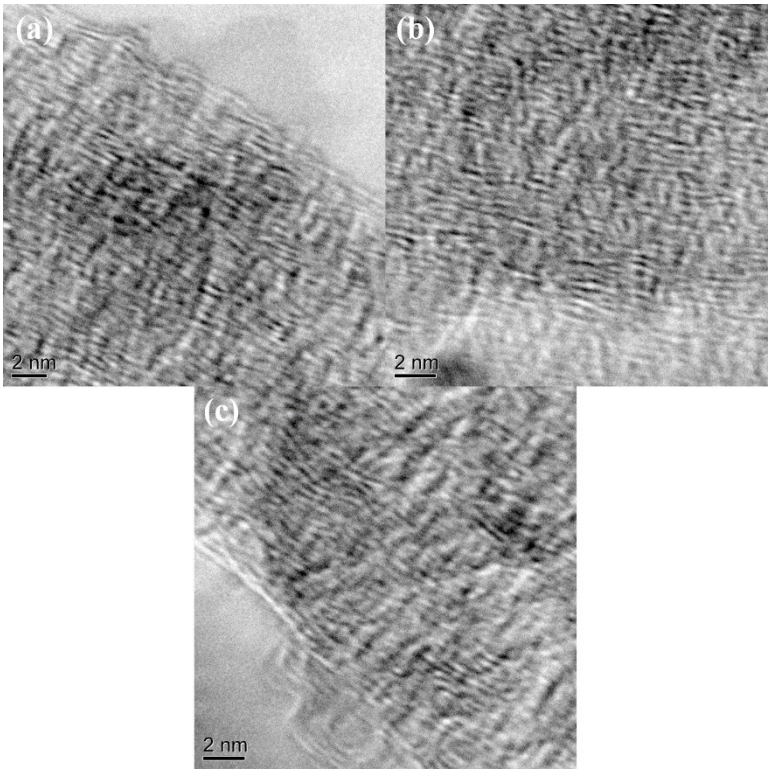

Fig. S10 TEM of the DWFC-600 (a), DWFC-1000 (b) and DWFC-1200 (c) flexible electrode material.

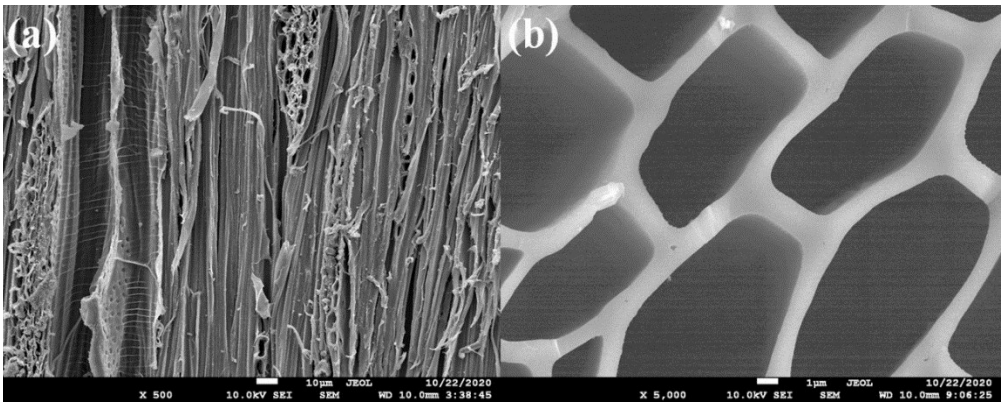

Fig. S11 SEM of the undelignified wood-based carbon material.

The carbon yield of the undelignified wood-based carbon material is about 31% at 800 ^{o}C.

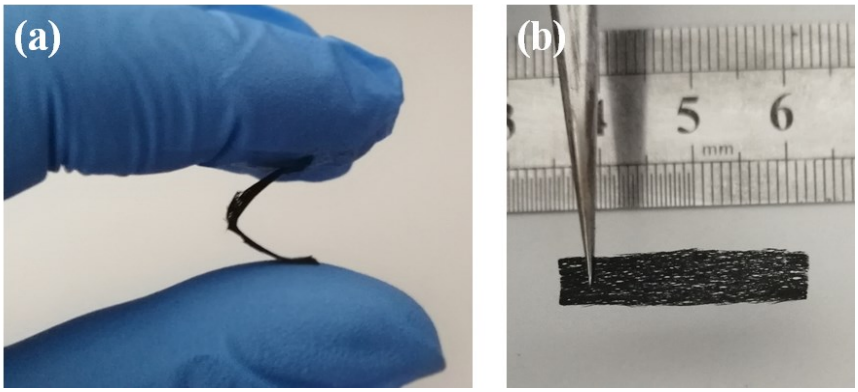

Fig. S12 Flexibility of the DWFC-800 flexible electrode material (a), the DWFC-800 flexible electrode material after bending (b).

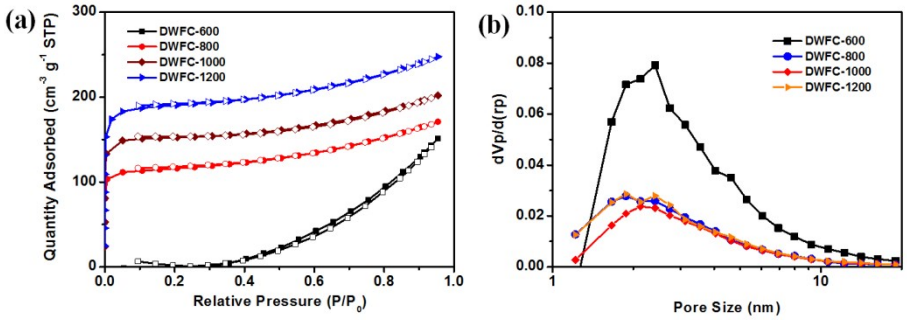

Fig. S13 Nitrogen adsorption/desorption isotherms (a) and BJH pore-size distribution (b) of the delignified wood-based carbon materials.

Table S4 The specific surface area of the DWFC-X carbon materials

Sample	DWFC-600	DWFC-800	DWFC-1000	DWFC-1200
S_{BET}(m^2 g^{-1})	37	460	615	756

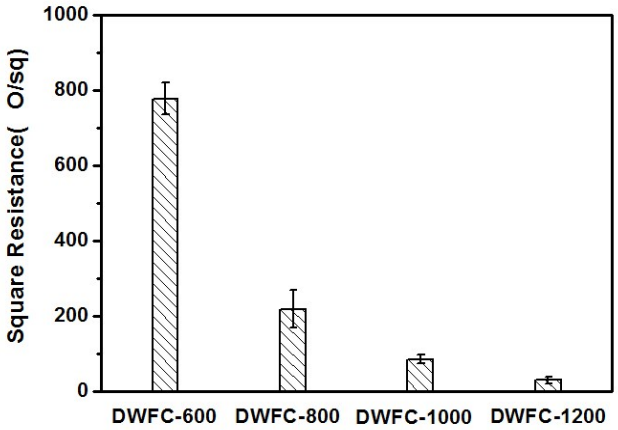

Fig. S14 The sheet resistance of the delignified wood-based carbon materials.

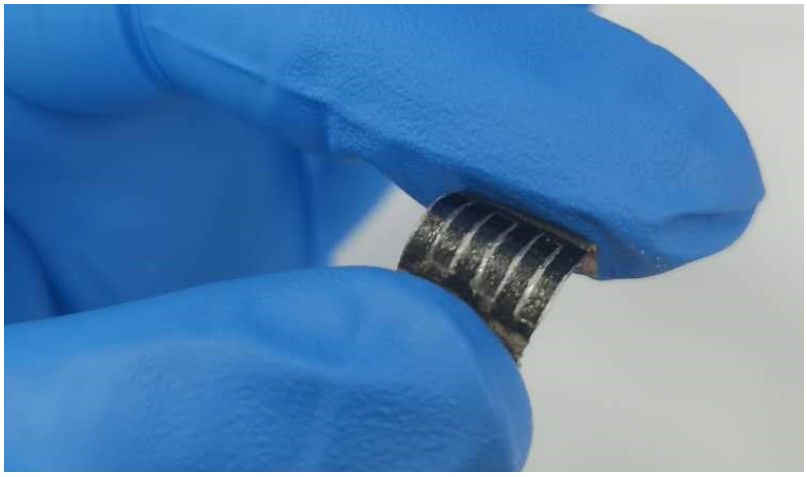

Fig. S15 The DWFC-800 based flexible self-supporting interdigitated solid supercapacitor.

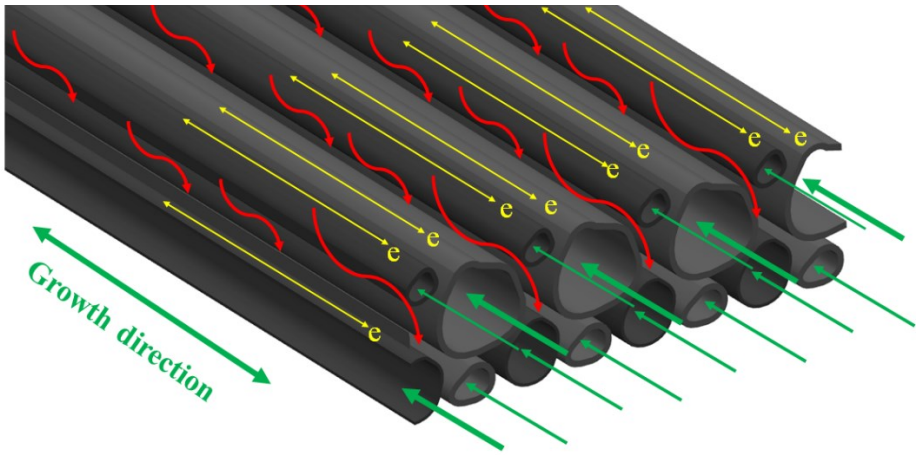

Fig. S16 Illustration of the penetration path for electrolyte and transmission path of electrons.

The electrolyte penetration path of the sandwich structure is mainly the schematic path of the red penetration. However, the electrolyte penetration path of the interdigitated structure is the schematic path of the red and green penetration. The transmission path of electrons is the yellow schematic path.

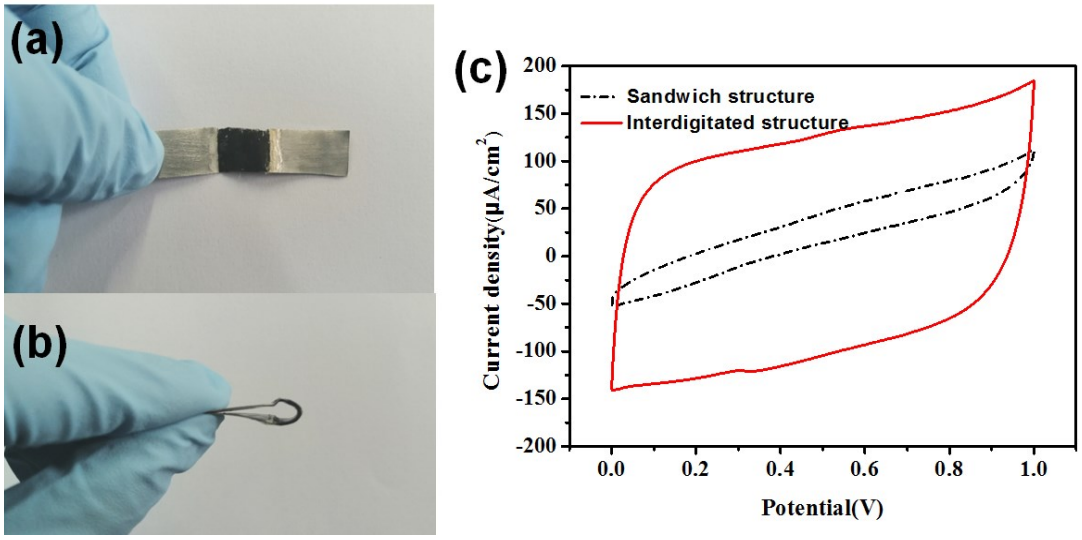

Fig. S17 The DWFC-800 based flexible solid supercapacitors with sandwich structure (a and b), the CV curves of the DWFC-800 based flexible self-supporting solid supercapacitors with sandwich structure and interdigitated structure at 5 mV/s (c).

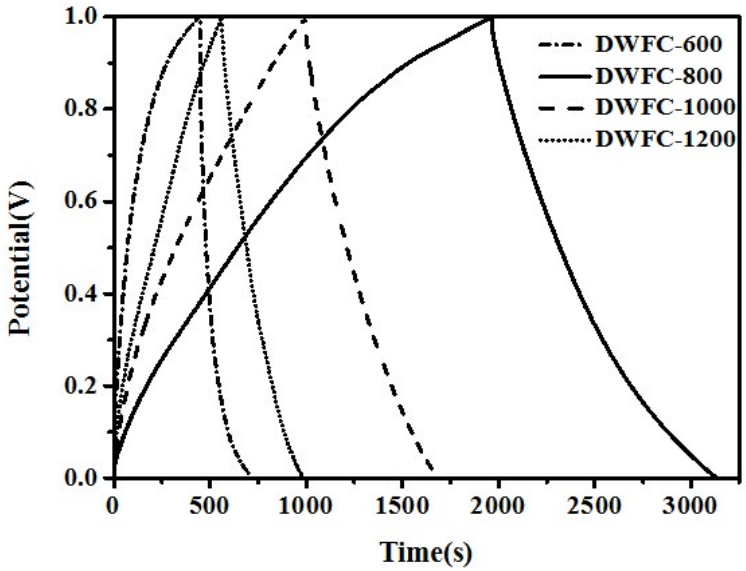

Fig. S18 The GCD curves of the DWFC-X based flexible self-supporting interdigital solid supercapacitor at a current density of 20 μA cm^{-2}.

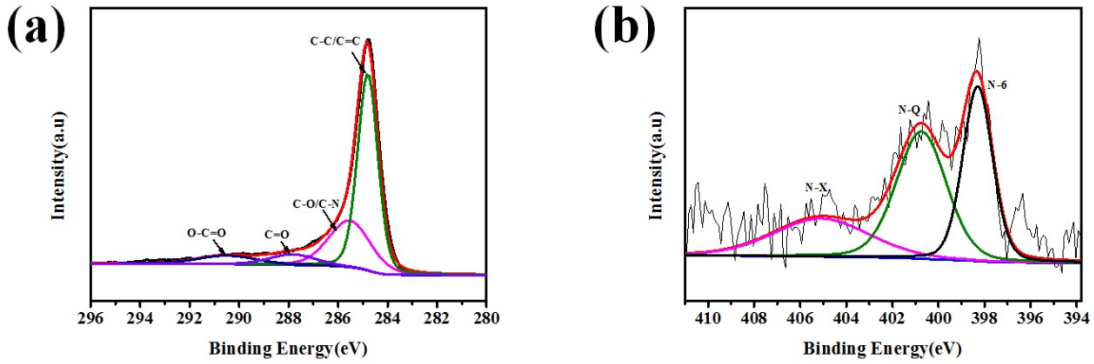

Fig. S19 High resolution C1s and N 1s XPS spectra of the DWFC-800 flexible electrode material.

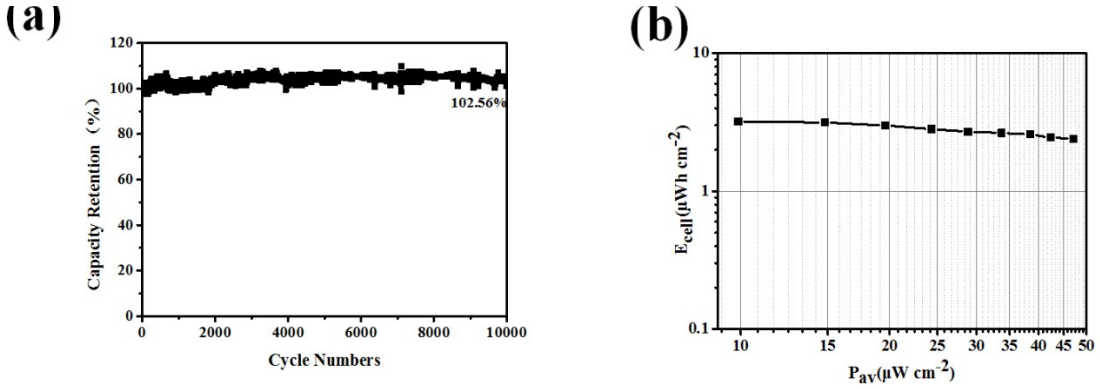

Fig. S20 Cycling stability of the DWFC-800 based flexible self-supporting interdigital solid supercapacitor at a current density of 400 μA cm^{-2} up to 10 000 cycles (a); Ragone plot of the DWFC-800 based flexible self-supporting interdigital solid supercapacitor (b)

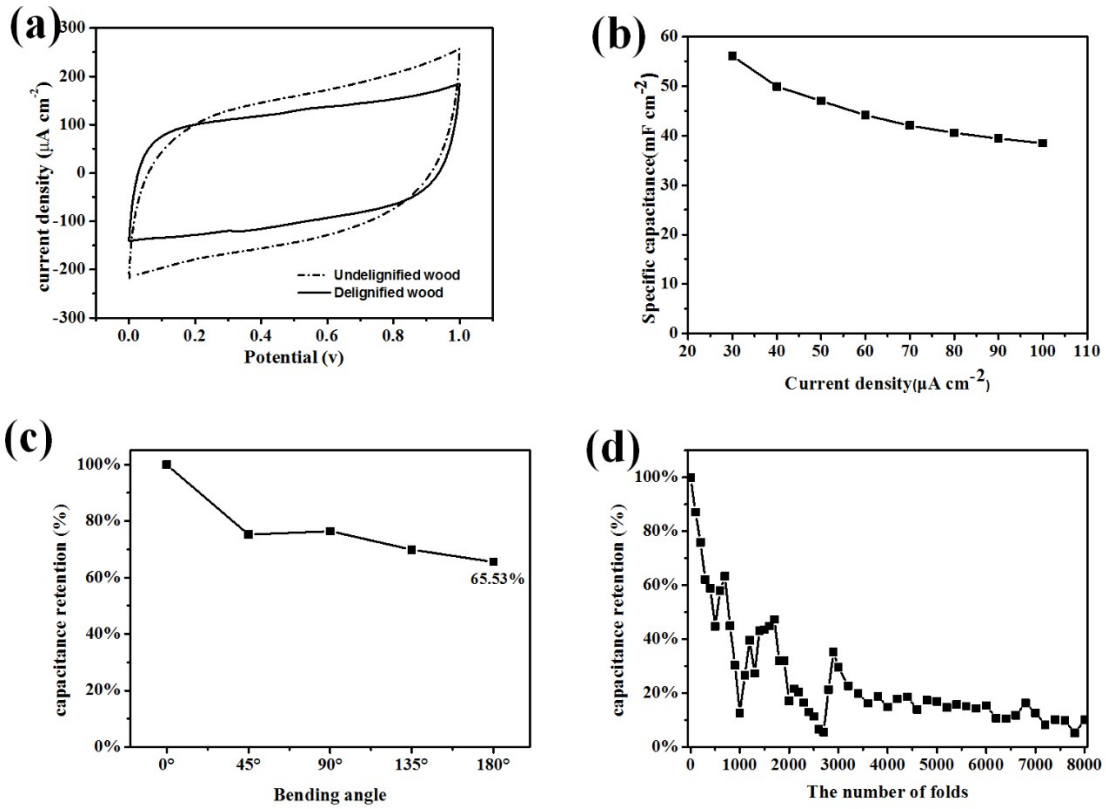

Fig. S21 The CV curves of the undelignified wood carbon-based interdigital solid supercapacitor and DWFC-800 based flexible self-supporting interdigital solid supercapacitor at 5 mV/s (a); the areal capacitance of the undelignified wood carbon-based interdigital solid supercapacitor at different current densities (b); the capacitance retention of the undelignified wood carbon-based interdigital solid supercapacitor at different bending angle (C); the capacitance retention of the undelignified wood carbon-based interdigital solid supercapacitora at different fold times.

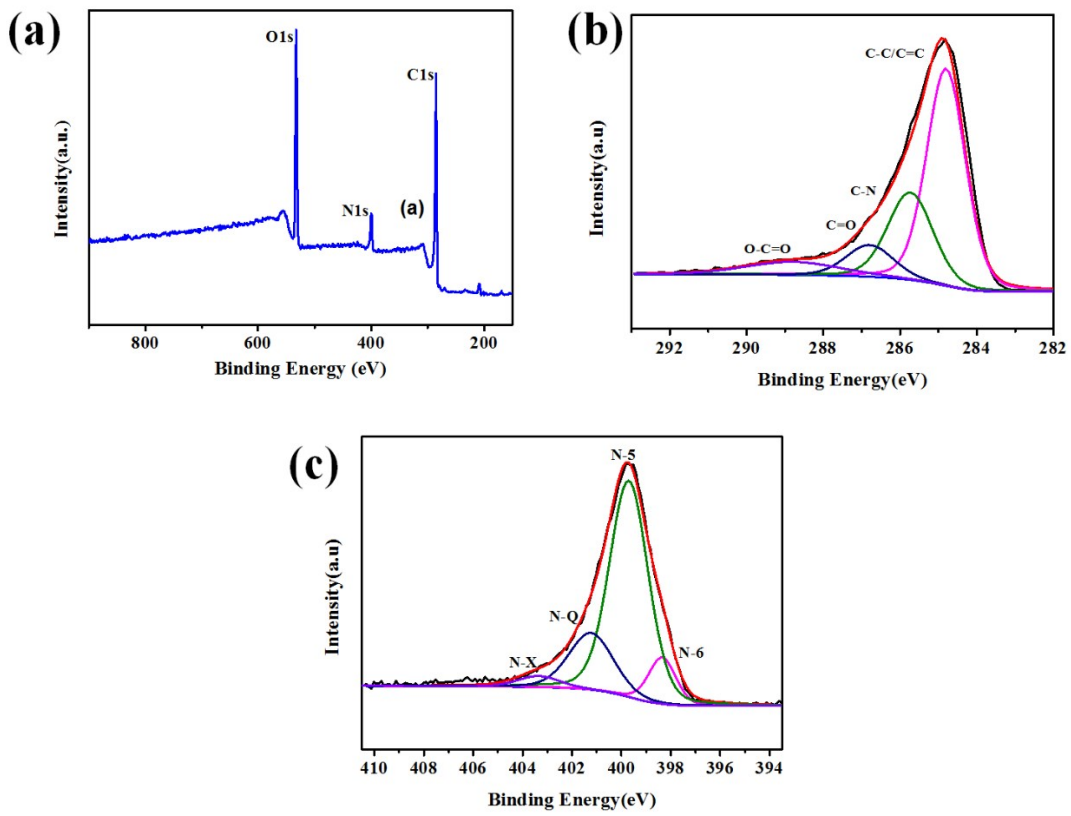

Fig. S22 XPS survey spectrum (a) and high-resolution XPS spectra of C 1s (d), N 1s (e) of the DWCPA-1.00 electrode material.

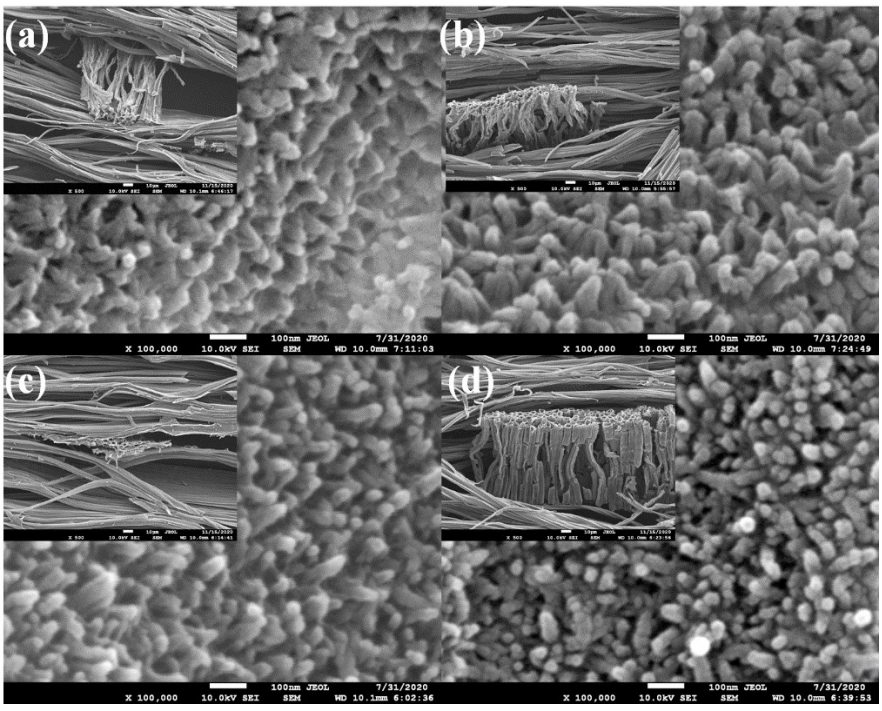

Fig. S23 SEM of the DWCPA-0.25, DWCPA-0.5, DWCPA-1 and DWCPA-2 electrode material.

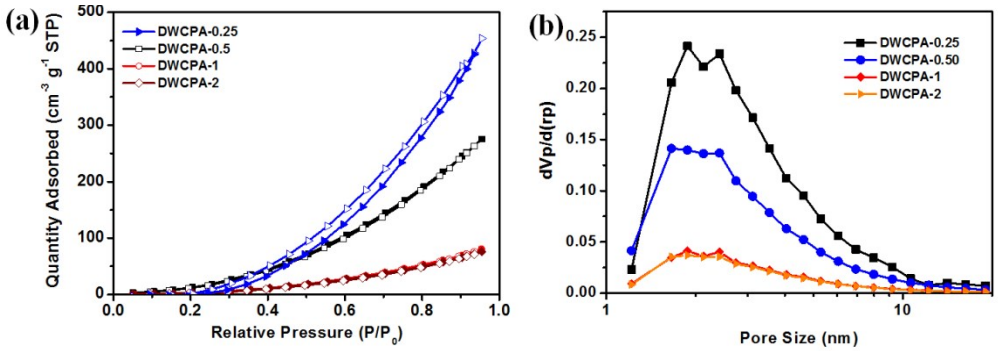

Fig. S24 Nitrogen adsorption/desorption isotherms (a) and BJH pore-size distribution (b) of the DWCPA-X composite materials.

Table S5 The specific surface area of the DWCPA-X carbon materials

Sample	DWCPA-0.25	DWCPA-0.5	DWCPA-1	DWCPA-2
S_{BET}(m^2 g^{-1})	168	140	35	34

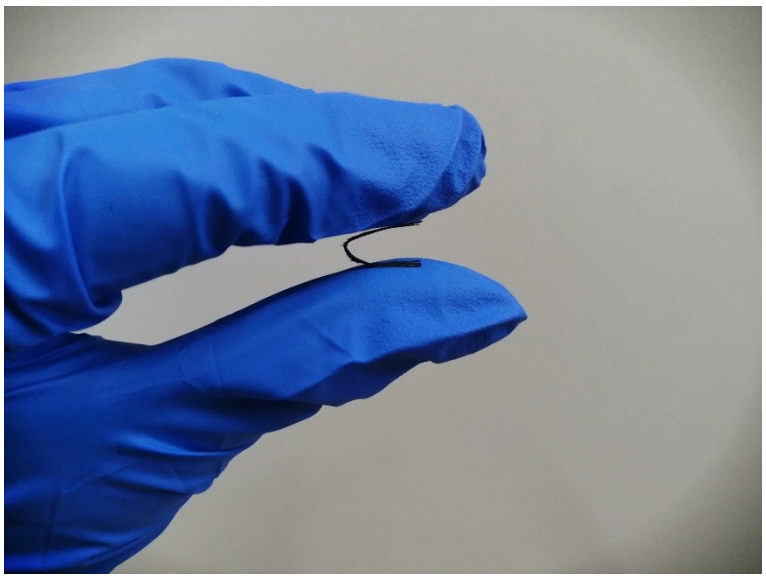

Fig. S25 The DWCPA-1 flexible electrode material.

Table S6 Thickness of the DWCPA-X flexible electrode material

sample	DWCPA-0.25	DWCPA-0.5	DWCPA-1	DWCPA-2
Thickness	40 μm	44μm	42μm	38μm

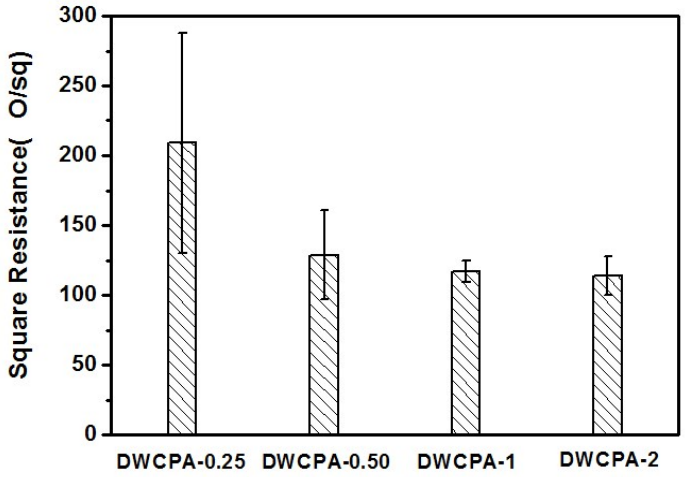

Fig. S26 The sheet resistance of the delignified wood-based carbon/polyaniline nanowire arrays composite materials.

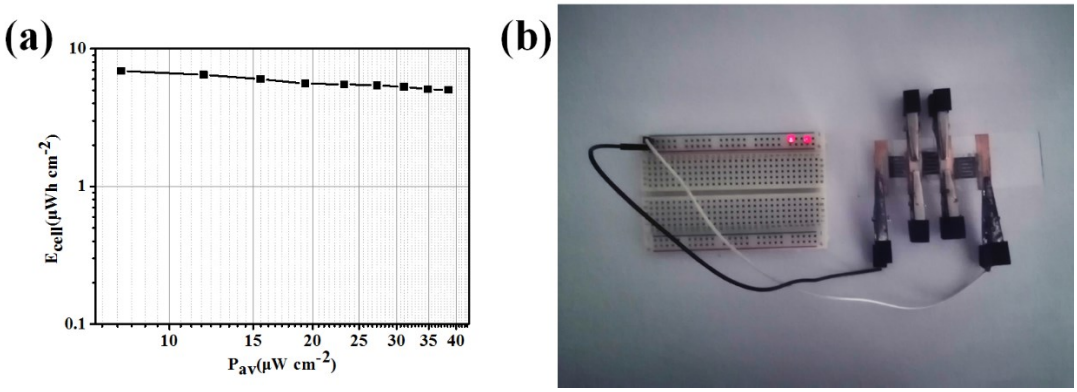

Fig. S27 Ragone plot of the DWCPA-1 based flexible self-supporting interdigital solid supercapacitor (a), Three DWCPA-1-based flexible self-supporting interdigitated solid supercapacitors in series can light up two red LED lamps.